Plane Coutte-Poiseuille Flow of Power-Law Non-Newtonian Fluids

by

Ganbat DAVAA*, Toru SHIGECHI** and Satoru MOMOKI**

The fully developed laminar flow of a non-Newtonian fluid flowing between two parallel plates with one moving plate was studied analytically. Applying the shear stress described by the power-law model, the exact solutions for the momentum equation were obtained.

The effects of the velocity of a moving plate and the flow index of a non-Newtonian power-law fluid on the velocity distribution and friction factor have been discussed.

1. Introduction

Problems involving fluid flow and heat transfer with an axially moving core of solid body or fluid in an annular geometry can be found in many manufacturing processes, such as extrusion, drawing and hot rolling, etc. In such processes, a hot plate or cylindrical rod continuously exchanges heat with the surrounding environment. For such cases, the fluid involved may be Newtonian or non-Newtonian and the flow situations encountered can be either laminar or turbulent.

In the previous report[1], fully developed laminar heat transfer of a Newtonian fluid flowing between two parallel plates with one moving plate was analyzed taking into account the viscous dissipation of the flowing fluid.

In engineering applications such as manufacturing processes, many important fluids are non-Newtonian in their flow characteristics.

In this paper, an exact solution of the momentum equation is obtained for fully developed laminar flow of a non-Newtonian fluid flowing between two parallel plates with one moving plate. The constitutive equation (i.e., the shear stress - shear rate relation) for a non-Newtonian fluid is described by the power-law model most frequently used in non-Newtonian fluid flow and heat transfer. The effects of the relative velocity of a moving plate and the flow index of a power-law fluid on the velocity distribution and friction factor have been discussed.

Nomenclature

C	integration constant
p	pressure
u	axial velocity of fluid
u^*	dimensionless velocity $\equiv u/u_m$
u_m	average velocity of fluid
U	axial velocity of the moving plate
U^*	relative velocity of the moving plate
y	coordinate normal to the fixed plate
y^*	dimensionless coordinate $\equiv y/L$
z	axial coordinate
ρ	density
L	channel width
m	consistency index
n	flow index
f	friction factor
F	dimensionless parameter
Re^*	generalized Reynolds number

Subscripts

0 fixed plate

L moving plate

2. Analysis

The physical model for the analysis is shown in Fig.1. The assumptions and conditions used

Received on October 26, 1999

* Graduate Student, Department of Mechanical Systems Engineering

**Department of Mechanical Systems Engineering

in the analysis are:

1. The flow is incompressible and steady-laminar, and hydrodynamically fully developed.
2. The fluid is non-Newtonian and the shear stress may be described by the power-law model, and physical properties are constant.
3. Either of two parallel plates is axially moving at a constant velocity.

The governing momentum equation together with the assumptions described above is

$$\frac{d\tau}{dy} = -\frac{dp}{dz} \tag{1}$$

The boundary conditions are:

$$\begin{cases} u = 0 \text{ at } y = 0 \\ u = U \text{ at } y = L \end{cases} \tag{2}$$

The shear stress on the left hand side of Eq.(1) τ, is given by the power-law model.

$$\tau = -m\left|\frac{du}{dy}\right|^{n-1}\frac{du}{dy} \tag{3}$$

For a Newtonian fluid, $n = 1$ and m coincides with the ordinary viscosity.

The friction factor, f, and generalized Reynolds number, Re^*, are defined as

$$f \equiv \frac{L}{\rho u_m^2}\left(-\frac{dp}{dz}\right) \tag{4}$$

$$Re^* \equiv \frac{\rho u_m^{2-n}(2L)^n}{m} \tag{5}$$

The average fluid velocity, u_m, is defined as

$$u_m \equiv \frac{1}{L}\int_0^L u dy \tag{6}$$

The following dimensionless parameters are introduced:

$$y^* \equiv y/L \tag{7}$$

$$u^* \equiv u/u_m \tag{8}$$

$$U^* \equiv U/u_m \tag{9}$$

$$L^*_{max} \equiv L_{max}/L \tag{10}$$

For the case with a moving plate, two kinds of velocity profiles across the parallel plates' passage may be assumed as illustrated in Figs.1 and 2. The velocity profile shown in Fig.1 has a maximum at $y = L_{max}$ whereas it has no maximum point in Fig.2. The two cases are respectively referred to as Case I and Case II.

Case I: The shear stress is calculated as

$$\tau = -m\left(\frac{du_a}{dy}\right)^n \quad (0 \leqq y \leqq L_{max}) \tag{11}$$

$$\tau = m\left(-\frac{du_b}{dy}\right)^n \quad (L_{max} \leqq y \leqq L) \tag{12}$$

(a) $0 \leqq y \leqq L_{max}$ $\quad 0 \leqq y^* \leqq L^*_{max}$

The momentum equation and its boundary conditions are reduced to

$$\frac{d}{dy^*}\left(\frac{du_a^*}{dy^*}\right)^n = -F \tag{13}$$

$$u_a^* = 0 \text{ at } y^* = 0 \tag{14}$$

where F is a parameter defined as

$$\frac{f \cdot Re^*}{2} = \frac{L^{n+1}}{m \cdot u_m^n}\left(-\frac{dp}{dz}\right) \equiv F \tag{15}$$

Since the velocity gradient is zero at the location of maximum velocity,

$$\frac{du_a^*}{dy^*} = 0 \text{ at } y^* = L^*_{max} \tag{16}$$

The integration of Eq.(13) together with Eq.(16) gives

$$\frac{du_a^*}{dy^*} = F^{\frac{1}{n}}(L^*_{max} - y^*)^{\frac{1}{n}} \tag{17}$$

Integrating Eq.(17) together with Eq.(14), we have

$$u_a^* = \frac{n}{1+n}F^{\frac{1}{n}}\left[L_{max}^{*\frac{1+n}{n}} - (L^*_{max} - y^*)^{\frac{1+n}{n}}\right] \tag{18}$$

(b) $L_{max} \leqq y \leqq L$ $\quad (L^*_{max} \leqq y^* \leqq 1)$

The momentum equation and its boundary conditions are reduced to

$$\frac{d}{dy^*}\left(-\frac{du_b^*}{dy^*}\right)^n = F \tag{19}$$

$$u_b^* = U^* \text{ at } y^* = 1 \tag{20}$$

Since the velocity gradient is zero at the location of maximum velocity,

$$\frac{du_b^*}{dy^*} = 0 \text{ at } y^* = L^*_{max} \tag{21}$$

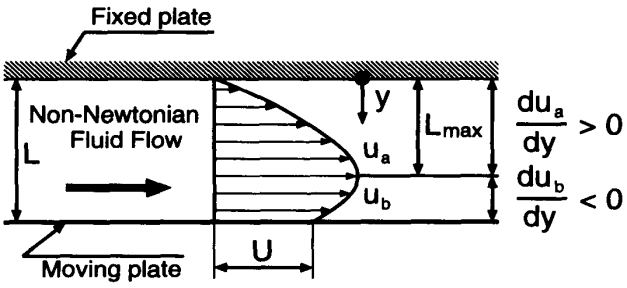

Fig.1 Schematic of parallel plates with one moving plate for the case of velocity profiles assumed in this analysis (Case I)

The integration of Eq.(19) together with Eq.(21) gives

$$\frac{du_b^*}{dy^*} = -F^{\frac{1}{n}}(y^*-L_{max}^*)^{\frac{1}{n}} \tag{22}$$

Integrating Eq.(22) together with Eq.(20), we have

$$u_b^* = U^* + \frac{n}{1+n}F^{\frac{1}{n}}\left[(1-L_{max}^*)^{\frac{1+n}{n}} - (y^*-L_{max}^*)^{\frac{1+n}{n}}\right] \tag{23}$$

The values of F and L_{max}^* remain unknown. They are determined below.

From the continuity of velocities at the location of maximum velocity:

$$u_a^* = u_b^* \quad \text{at} \quad y^* = L_{max}^* \tag{24}$$

we have the first relationship between F and L_{max}^*.

$$F = \left[\frac{U^*}{\frac{n}{1+n}\left\{L_{max}^{*\frac{1+n}{n}} - (1-L_{max}^*)^{\frac{1+n}{n}}\right\}}\right]^n \tag{25}$$

From the mass balance between two plates:

$$\int_0^1 u^*dy^* = \int_0^{L_{max}^*} u_a^*dy^* + \int_{L_{max}^*}^1 u_b^*dy^* = 1 \tag{26}$$

we have the second relationship between F and L_{max}^*.

$$F = \left[\frac{1-(1-L_{max}^*)U^*}{\frac{n}{1+2n}\left\{L_{max}^{*\frac{1+2n}{n}} + (1-L_{max}^*)^{\frac{1+2n}{n}}\right\}}\right]^n \tag{27}$$

Combining Eq.(25) and Eq.(27), we have the following relationship among U^*, L_{max}^* and n.

$$U^* = \left[L_{max}^{*\frac{1+n}{n}} - (1-L_{max}^*)^{\frac{1+n}{n}}\right] \Big/ \left[L_{max}^{*\frac{1+n}{n}} - \frac{n}{1+2n}\left\{L_{max}^{*\frac{1+2n}{n}} + (1-L_{max}^*)^{\frac{1+2n}{n}}\right\}\right] \tag{28}$$

Case II: The shear stress is calculated as

$$\tau = -m\left(\frac{du}{dy}\right)^n \quad (0 \leqq y \leqq L) \tag{29}$$

The momentum equation and its boundary conditions are reduced to

$$\frac{d}{dy^*}\left(\frac{du^*}{dy^*}\right)^n = -F \tag{30}$$

$$\begin{cases} u^* = 0 & \text{at } y^* = 0 \\ u^* = U^* & \text{at } y^* = 1 \end{cases} \tag{31}$$

Integrating Eq.(30), we have

$$\frac{du^*}{dy^*} = F^{\frac{1}{n}}(C-y^*)^{\frac{1}{n}} \tag{32}$$

The integration of Eq.(32) gives

$$u^* = \frac{n}{1+n}F^{\frac{1}{n}}\left[C^{\frac{1+n}{n}} - (C-y^*)^{\frac{1+n}{n}}\right] \tag{33}$$

where C is an integral constant. Applying the boundary conditions of Eq.(31) to Eq(33), we have

$$U^* = \frac{n}{1+n}F^{\frac{1}{n}}\left[C^{\frac{1+n}{n}} - (C-1)^{\frac{1+n}{n}}\right] \tag{34}$$

From the mass balance between two plates:

$$\int_0^1 \left[\frac{n}{1+n}F^{\frac{1}{n}}\left\{C^{\frac{1+n}{n}} - (C-y^*)^{\frac{1+n}{n}}\right\}\right]dy^* = 1 \tag{35}$$

Integrating Eq.(35), we have

$$\frac{n}{1+n}F^{\frac{1}{n}}\left[C^{\frac{1+n}{n}} + \frac{n}{1+2n}\left\{(C-1)^{\frac{1+2n}{n}} - C^{\frac{1+2n}{n}}\right\}\right] = 1 \tag{36}$$

thus, F is obtained as

$$F = \left[1\Big/\frac{n}{1+n}\left[C^{\frac{1+n}{n}} + \frac{n}{1+2n}\left\{(C-1)^{\frac{1+2n}{n}} - C^{\frac{1+2n}{n}}\right\}\right]\right]^n \tag{37}$$

Combining Eq.(34) and Eq.(37), we have the following relationship among C, n, and U^*.

$$U^* = \left[C^{\frac{1+n}{n}} - (C-1)^{\frac{1+n}{n}}\right] \Big/ \left[C^{\frac{1+n}{n}} + \frac{n}{1+2n}\left\{(C-1)^{\frac{1+2n}{n}} - C^{\frac{1+2n}{n}}\right\}\right] \tag{38}$$

The numerical values of L_{max}^* for the Case I and C for the Case II are calculated and given, respectively, in Tables 1 and 2. U_{cr}^* is a critical value that shows the border between Case I and Case II, and given, from Eq.(28) with $L_{max}^*=1$ as

$$U_{cr}^* = \frac{1+2n}{1+n} \tag{39}$$

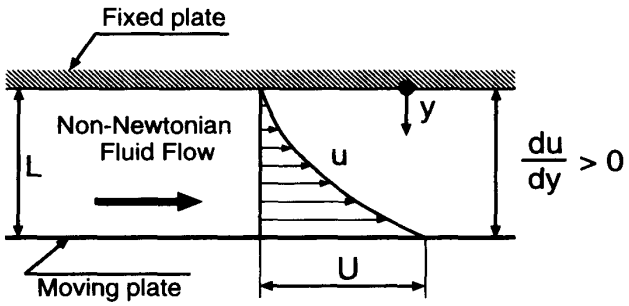

Fig.2 Velocity profile assumed in this analysis (Case II)

Teble 1 Dimensionless location at the maximum velocity, L^*_{max}

CASE I: L^*_{max}									
n	U^*								
	-2.0	-1.5	-1.0	-0.5	0.0	0.5	1.0	1.5	U^*_{cr}
0.1	0.4776	0.4812	0.4857	0.4916	0.5000	0.5143	0.5681	-	1.0909
0.2	0.4621	0.4681	0.4756	0.4856	0.5000	0.5244	0.5987	-	1.1667
0.3	0.4509	0.4585	0.4681	0.4811	0.5000	0.5319	0.6178	-	1.2308
0.4	0.4424	0.4511	0.4624	0.4777	0.5000	0.5376	0.6311	-	1.2857
0.5	0.4358	0.4454	0.4578	0.4749	0.5000	0.5422	0.6409	-	1.3333
0.6	0.4305	0.4407	0.4542	0.4726	0.5000	0.5458	0.6484	-	1.3750
0.7	0.4261	0.4369	0.4511	0.4708	0.5000	0.5489	0.6544	-	1.4118
0.8	0.4224	0.4337	0.4485	0.4692	0.5000	0.5515	0.6592	-	1.4444
0.9	0.4193	0.4309	0.4463	0.4678	0.5000	0.5537	0.6633	-	1.4737
1.0	0.4167	0.4286	0.4444	0.4667	0.5000	0.5556	0.6667	1.0000	1.5000
1.1	0.4144	0.4265	0.4428	0.4656	0.5000	0.5572	0.6696	0.9719	1.5238
1.2	0.4123	0.4247	0.4413	0.4647	0.5000	0.5587	0.6721	0.9521	1.5455
1.3	0.4106	0.4231	0.4401	0.4639	0.5000	0.5599	0.6743	0.9378	1.5652
1.4	0.4090	0.4217	0.4389	0.4632	0.5000	0.5611	0.6762	0.9270	1.5833
1.5	0.4076	0.4205	0.4379	0.4626	0.5000	0.5621	0.6780	0.9187	1.6000
1.6	0.4063	0.4193	0.4370	0.4620	0.5000	0.5630	0.6795	0.9121	1.6154
1.7	0.4051	0.4183	0.4361	0.4615	0.5000	0.5639	0.6809	0.9068	1.6296
1.8	0.4041	0.4174	0.4354	0.4610	0.5000	0.5646	0.6822	0.9024	1.6429
1.9	0.4031	0.4165	0.4347	0.4606	0.5000	0.5653	0.6833	0.8987	1.6552
2.0	0.4022	0.4157	0.4340	0.4601	0.5000	0.5660	0.6843	0.8956	1.6667

Teble 2 Integration constant C for Case II

CASE II: C						
n	U^*					
	1.5	1.6	1.7	1.8	1.9	1.99
0.1	5.0905	6.8662	9.7352	15.3693	32.1050	332.1608
0.2	2.7738	3.6681	5.1075	7.9285	16.2996	166.3301
0.3	2.0082	2.6071	3.5685	5.4504	11.0322	111.0533
0.4	1.6306	2.0805	2.8016	4.2130	8.3993	83.4150
0.5	1.4082	1.7676	2.3437	3.4720	6.8201	66.8321
0.6	1.2637	1.5617	2.0402	2.9790	5.7679	55.7768
0.7	1.1638	1.4169	1.8250	2.6279	5.0168	47.8803
0.8	1.0920	1.3104	1.6650	2.3654	4.4538	41.9579
0.9	1.0391	1.2295	1.5418	2.1620	4.0163	37.3516
1.0	1.0000	1.1667	1.4444	2.0000	3.6667	33.6667

3. Results and Discussion

Figure 3 shows the effects of the relative velocity of the moving plate U^* on the velocity profiles across the parallel plates for the cases of n = 0.2, 0.5, 1.0 and 1.5. The case of n = 1 corresponds to that of a Newtonian fluid. It is seen clearly in the figures that the profiles of the fluid velocity are deformed by the moving plate with a relative velocity U^*.

Figure 4 shows the effects of the flow index n of the power-law fluid on the velocity profiles across the parallel plates for the cases of U^* = -1.5, 0, 1.0 and 1.5. The case of U^* = 0 corresponds to that of both plates fixed. It is seen in the figures that for $U^* < 0$ the velocity profile is parabolic having a larger maximum value with increasing values of n. The velocity profiles are strongly affected by the flow index n. For $U^* > 0$ the velocity profiles become linear as the effect of the axial pressure gradient in the fluid diminishes and the fluid flow is governed only by the shear flow induced by the moving plate. In this case, the effect of n is rather weak.

The predicted friction factors in terms of ,

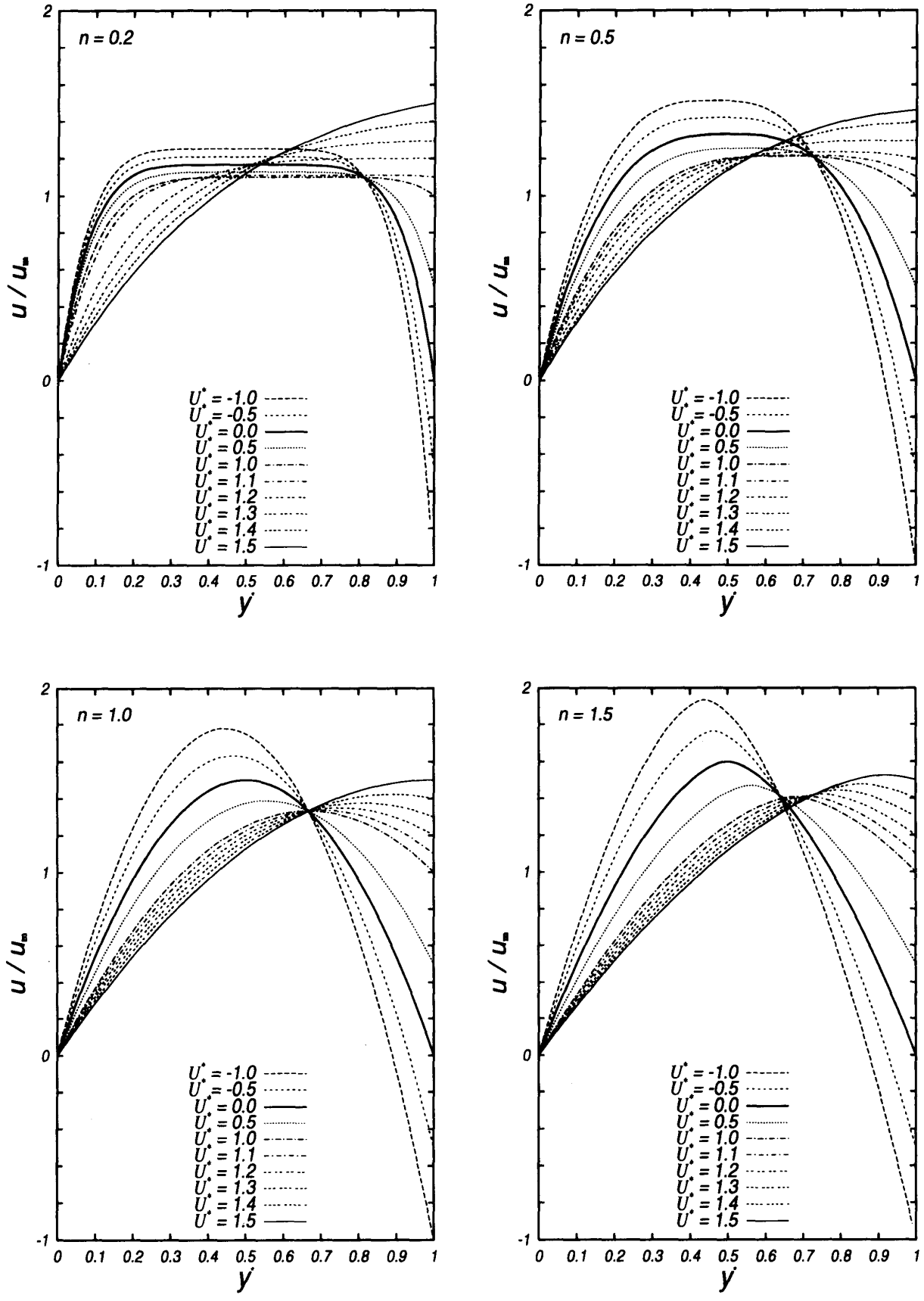

Fig. 3 Velocity profile

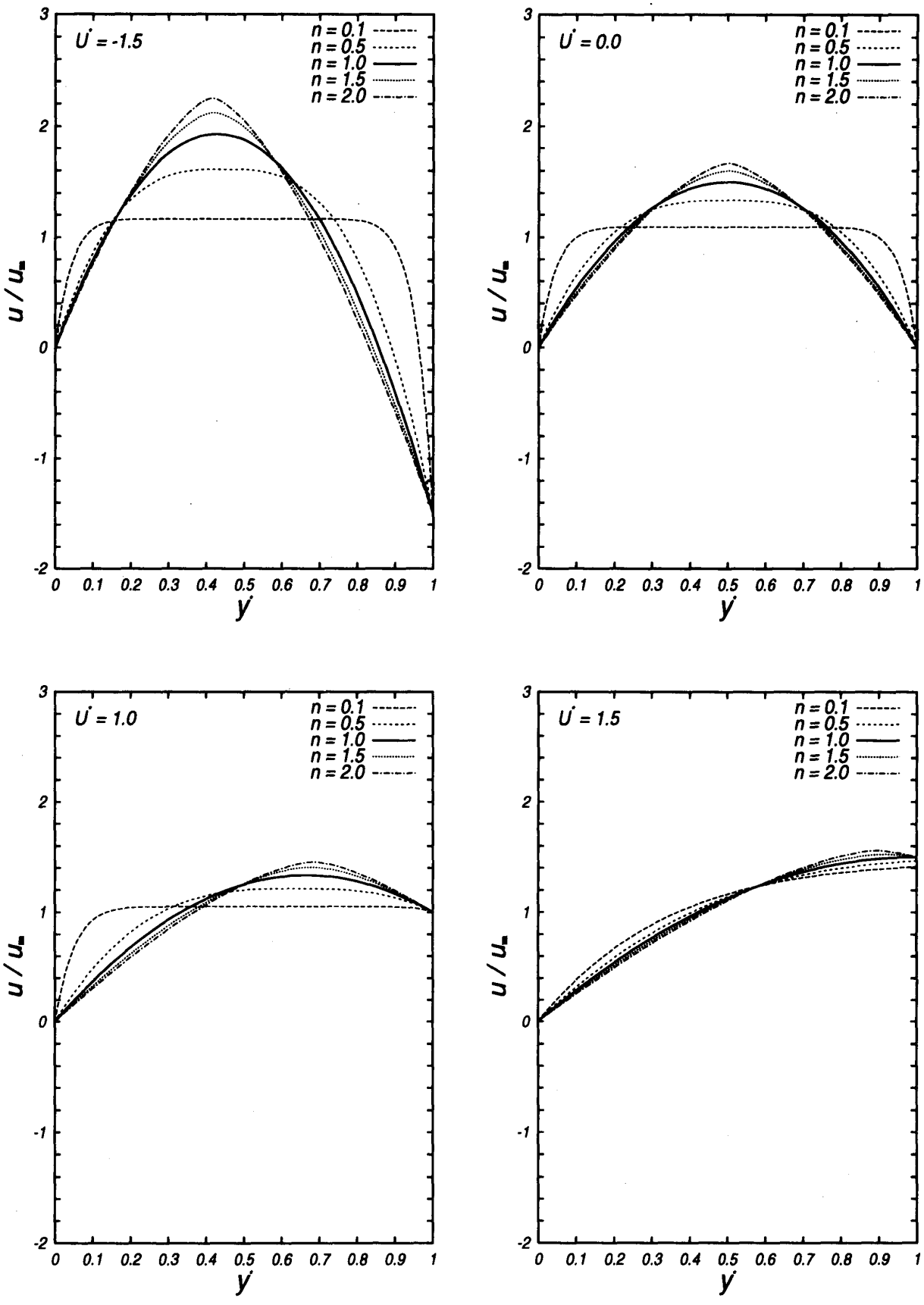

Fig. 4 Velocity profile

fRe^* are shown in Fig.5. The effect of n is to increase the value of fRe^* with an increase in n.

Figure 6 shows the effect of n on fRe^*, normalized by the value of $fRe^*_{(U^*=0)}$ for the case of $U^* = 0$. For $U^* > 0$, the ratio $fRe^*/fRe^*_{(U^*=0)}$ is always less than unity. The effect of U^* becomes stronger in the region of larger values of

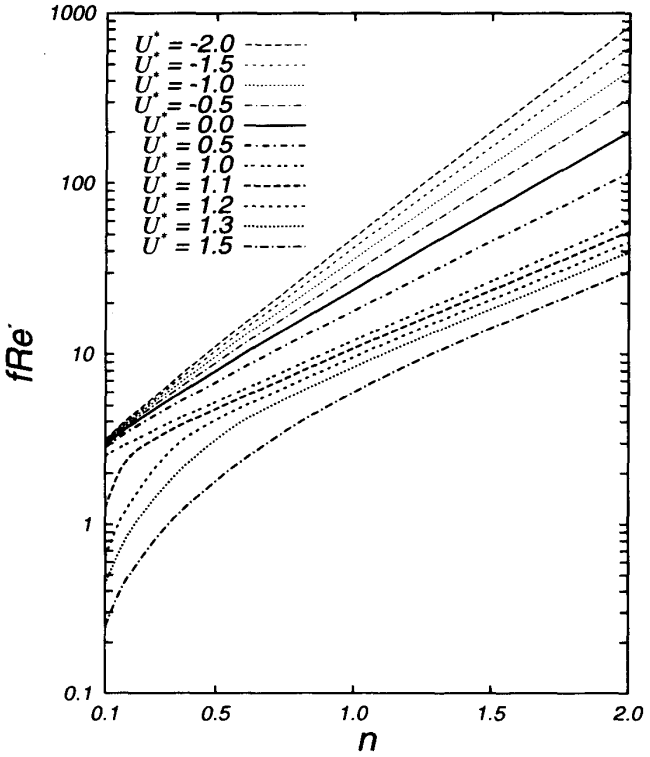

Fig. 5 Friction factor

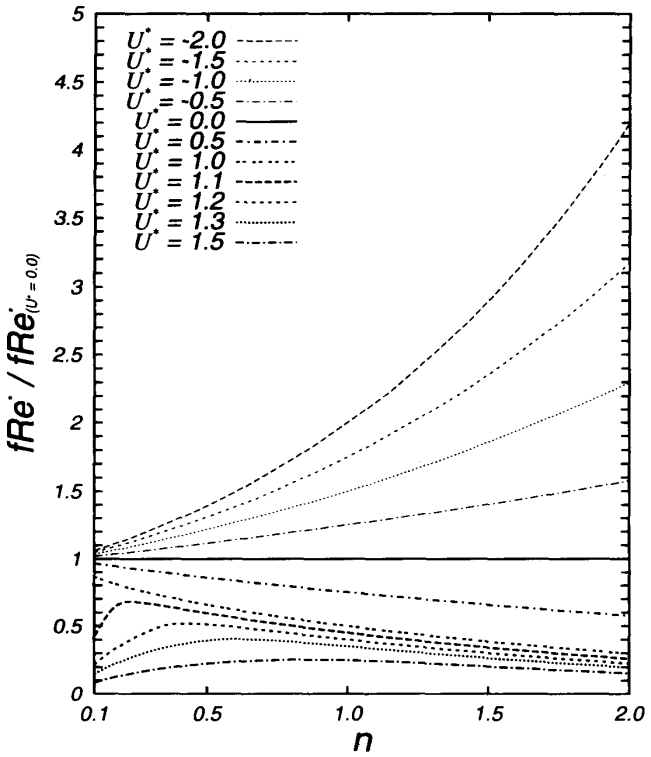

Fig. 6 Friction factor ratio

Teble 3 Numerical values of fRe^*

fRe^*								
n	U^*							
	-2.0	-1.5	-1.0	-0.5	0.0	0.5	1.0	1.5
0.1	3.1241	3.0919	3.0540	3.0073	2.9455	2.8495	2.5503	0.2480
0.2	4.4048	4.3075	4.1959	4.0629	3.8946	3.6527	3.1007	0.5378
0.3	6.0599	5.8503	5.6146	5.3416	5.0090	4.5605	3.7205	0.8858
0.4	8.2406	7.8496	7.4181	6.9300	6.3553	5.6218	4.4333	1.3037
0.5	11.1321	10.4591	9.7291	8.9218	8.0000	6.8795	5.2599	1.8042
0.6	14.9754	13.8747	12.7006	11.4294	10.0191	8.3793	6.2228	2.4003
0.7	20.0886	18.3505	16.5268	14.5924	12.5041	10.1735	7.3471	3.1057
0.8	26.8932	24.2185	21.4569	18.5856	15.5663	12.3238	8.6615	3.9336
0.9	35.9491	31.9124	27.8108	23.6291	19.3423	14.9035	10.1995	4.8958
1.0	48.0000	42.0000	36.0000	30.0000	24.0000	18.0000	12.0000	6.0000
1.1	64.0339	55.2245	46.5538	38.0477	29.7460	21.7181	14.1085	7.2492
1.2	85.3638	72.5590	60.1535	48.2129	36.8349	26.1833	16.5782	8.6596
1.3	113.7338	95.2770	77.6759	61.0515	45.5801	31.5462	19.4712	10.2619
1.4	151.4617	125.0460	100.2492	77.2647	56.3679	37.9873	22.8602	12.0926
1.5	201.6265	164.0486	129.3253	97.7373	69.6744	45.7234	26.8305	14.1928
1.6	268.3184	215.1240	166.7728	123.5849	86.0861	55.0145	31.4818	16.6084
1.7	356.9710	282.0658	214.9959	156.2151	106.3257	66.1727	36.9308	19.3912
1.8	474.8019	369.7145	277.0880	197.4031	131.2839	79.5726	43.3143	22.6007
1.9	631.3978	484.4938	357.0297	249.3883	162.0580	95.6637	50.7923	26.3046
2.0	839.4918	634.7873	459.9420	314.9947	200.000	114.9855	59.5522	30.5810

n ($n > 1.0$). The numerical values of fRe^* are given in Table 3.

4. Conclusion

The plane Coutte-Poiseuille flow of power-law non-Newtonian fluid was analysed.

The present study showed that for equal conditions:

1. The velocity profiles are strongly affected by the flow index, n, for the case of $U^* < 0$. In this case, the velocity profile is parabolic having a larger maximum value with increasing values of n. For the case of $U^* > 0$, the effect of n on the velocity is small and the profile becomes linear.
2. The friction factor in terms of fRe^* decreases with increasing values of U^*.

Reference

1. T. Shigechi, et al., *Reports of the Faculty of Engineering, Nagasaki University*, **29**, (1999-7), 153.